

EmoFace: Emotion-Content Disentangled Speech-Driven 3D Talking Face Animation

Yihong Lin¹, Liang Peng², Xianjia Wu², Jianqiao Hu¹, Xiandong Li^{2,*},
Wenxiong Kang^{1,*}, Songju Lei³ and Huang Xu²

¹South China University of Technology

²Huawei Cloud

³Nanjing University

lixiandong6@huawei.com, auwxkang@scut.edu.cn

Abstract

The creation of increasingly vivid 3D talking face has become a hot topic in recent years. Currently, most speech-driven works focus on lip synchronisation but neglect to effectively capture the correlations between emotions and facial motions. To address this problem, we propose a two-stream network called EmoFace, which consists of an emotion branch and a content branch. EmoFace employs a novel Mesh Attention mechanism to analyse and fuse the emotion features and content features. Particularly, a newly designed spatio-temporal graph-based convolution, SpiralConv3D, is used in Mesh Attention to learn potential temporal and spatial feature dependencies between mesh vertices. In addition, to the best of our knowledge, it is the first time to introduce a new self-growing training scheme with intermediate supervision to dynamically adjust the ratio of groundtruth adopted in the 3D face animation task. Comprehensive quantitative and qualitative evaluations on our high-quality 3D emotional facial animation dataset, 3D-RAVDESS (4.8863×10^{-5} mm for LVE and 0.9509×10^{-5} mm for EVE), together with the public dataset VOCASET (2.8669×10^{-5} mm for LVE and 0.4664×10^{-5} mm for EVE), demonstrate that our approach achieves state-of-the-art performance.

1 Introduction

Generating realistic 2D/3D face animations has received great attention in a number of fields, including film production, computer games, virtual reality, education, etc. [Ping *et al.*, 2013; Edwards *et al.*, 2016; Wohlgenannt *et al.*, 2020]. Recent methods based on deep learning [Karras *et al.*, 2017; Cudeiro *et al.*, 2019; Richard *et al.*, 2021; Fan *et al.*, 2022; Xing *et al.*, 2023; Peng *et al.*, 2023a; Wu *et al.*, 2023; Stan *et al.*, 2023] produce impressive 3D face animations with significant savings in time and labour compared to manual production, making them preferred for academic research and commercial exploration. However, there are still some situations remained to be adequately addressed, for example, the

relationship between emotions and facial expressions. Most of the preceding speech-driven methods [Cudeiro *et al.*, 2019; Richard *et al.*, 2021; Fan *et al.*, 2022; Xing *et al.*, 2023; Peng *et al.*, 2023a] focus more on achieving high-quality lip synchronisation, while ignoring the impact of emotion on facial animations. Recognizing the significance of emotion, EmoTalk [Peng *et al.*, 2023b] and EMOTE [Daněček *et al.*, 2023] disentangle emotional and content information in speech to generate high-quality emotional 3D facial animations. Nevertheless, EmoTalk only uses emotion as the driving source, regardless of content, thereby limiting its performance. EMOTE doesn't achieve end-to-end training and adopts a FLAME [Li *et al.*, 2017] parameter-based method that theoretically does not control motion as accurately as vertex-based methods because the abstract coefficient estimation ignores spatial correlations.

In this paper, we propose a novel vertex-based autoregressive emotional speech-driven 3D face animation approach. We first disentangle emotion and content from speech and extract their features separately, then a latent space decoder is used to obtain the emotion-based and content-based vertex offsets, which are eventually integrated by Mesh Attention to predict the final offsets. Due to that the fusion weights for the emotion branch and the content branch are variable in both temporal and spatial domains, we add a 3D graph-based convolution operator SpiralConv3D in Mesh Attention for effective feature exaction. Moreover, during the training process, it is observed that the autoregression scheme of the transformer decoder results in error accumulation, which ultimately leads to a deterioration in the output and increases the training time. Although, existing teacher-forcing scheme can help to alleviate this problem, exposure bias may occur when switching from training to inference due to inability to access real historical data. Inspired by scheduled sampling [Mihaylova and Martins, 2019], we propose a self-growing scheme that gradually adjusts the ratio of groundtruth provided during training. In order to better train our emotion-content disentanglement model, we construct a high-quality dataset 3D-RAVDESS by reconstructing reliable 3D faces from 2D dataset RAVDESS [Livingstone and Russo, 2018]. Extensive qualitative and quantitative experiments demonstrate that our method outperforms current state-of-the-art methods for better generation of facial expressions and lip synchronisation.

In summary, our main contributions are as follows:

- We provide a new high-quality emotional speech-driven dataset, 3D-RAVDESS.
- We design a two-stream network, EmoFace, to obtain the emotion-based and content-based vertex offsets, respectively, which are dynamically fused by a novel Mesh Attention with SpiralConv3D that efficiently extracts features in the spatio-temporal domain.
- We introduce intermediate supervision to guide two branches respectively and propose a self-growing training scheme to gradually increase the difficulty of prediction, thus improving the robustness of the model.
- Extensive experiments demonstrate the superiority of EmoFace over existing SOTA methods in terms of full face realism, emotion expression and lip synchronisation on both 3D-RAVDESS and VOCASET.

2 Related Work

2.1 Speech-Driven 3D Talking Face

Speech-driven 3D talking face generation is a task to generate realistic facial animations based on speech [Karras *et al.*, 2017; Lahiri *et al.*, 2021; Pham *et al.*, 2017; Taylor *et al.*, 2017]. A number of rule-based approaches have been employed to generate 3D motions, including the capture of the relationship between visemes [Mattheyses and Verhelst, 2015] and facial action units (FAUs) [Ekman and Friesen, 1978], as well as the establishment of a phoneme-viseme mapping that has yielded highly promising results in early studies [Edwards *et al.*, 2016; Xu *et al.*, 2013]. Nevertheless, these methods do not easily transfer to new faces as they heavily rely on manual crafting and consume an excessive amount of time.

In contrast to rule-based methods, deep learning-based 3D face animation methods resort to a data-driven framework. Most of them take both speech and a static 3D mesh template as input to generate realistic 3D face animations. In an early work, VOCA [Cudeiro *et al.*, 2019] proposes a temporal convolutional neural network with an open-source 4D dataset VOCASET, [Cudeiro *et al.*, 2019], which has become a valuable resource for subsequent studies. Building on this foundation, MeshTalk [Richard *et al.*, 2021], FaceFormer [Fan *et al.*, 2022], and CodeTalker [Xing *et al.*, 2023] incorporate motion priors to improve animation quality. MeshTalk notes the importance of facial motion in audio-uncorrelated regions and adopts categorical latent space to learn discrete motion priors. FaceFormer focuses on the long temporal sequences and successfully uses a transformer decoder [Vaswani *et al.*, 2017] to obtain contextual information to generate sequential mesh sequences. CodeTalker introduces VQ-VAE [Van Den Oord *et al.*, 2017] to learn discrete motion priors for smooth facial motion generation. More recently, SelfTalk [Peng *et al.*, 2023a] proposes consistency loss to improve the generation quality. Other works [Stan *et al.*, 2023; Chen *et al.*, 2023; Sun *et al.*, 2024] introduce diffusion model into 3D facial animation to enhance motion diversity.

However, all these approaches have mainly focused on lip synchronisation but have not paid attention to the correlation

between emotions and facial expressions. To address this problem, EmoTalk [Peng *et al.*, 2023b] and EMOTE [Daněček *et al.*, 2023] both propose speech-driven content-emotion disentanglement pipelines. Nevertheless, EmoTalk does not utilize content information and only focuses on the driving effect of emotional information, while the effectiveness and efficiency of EMOTE are limited by FLAME parameters and two-stage training pipelines, respectively.

2.2 Spiral Convolution

Defferrard *et al.* [Defferrard *et al.*, 2016] present a graph convolutional network (GCN) based on spectral filtering for non-Euclidean graph structure with the same linear complexity as the classical CNN. Kolotouros *et al.* [Kulon *et al.*, 2020] devise a simple model consisting of an encoder and a decoder with spiral convolution added to the decoder, which can directly learn the mapping relationships from 2D images to 3D meshes. However, the graph convolution operator is not intuitive enough for dealing with 3D mesh vertices in the spatial domain. Therefore, Masci *et al.* [Masci *et al.*, 2015] advance the idea of spatial graph convolution with sampling of the graph signal. Lim *et al.* [Lim *et al.*, 2018] propose spiral convolution based on graph convolution to handle 3D mesh vertices in the spatial domain. Gong *et al.* [Gong *et al.*, 2019] introduce SpiralNet++, which utilizes truncated spiral lines to constrain the number of sampled vertices, while incorporating hollow spiral lines to enhance the receptive field. Inspired by these previous works, we use spiral convolution in a 3D facial animation generation task to allow EmoFace to better learn the spatial as well as temporal associations of mesh vertices.

3 Methods

3.1 Overview

The overall pipeline is shown in Figure 1. In order to generate vivid emotional 3D talking faces, we propose EmoFace, a model that can sufficiently learn emotions from speech and generate talking face with rich expressions. The input of EmoFace consists of the speech sequence $A_{1:T} = (a_1, a_2, \dots, a_T)$, the emotional level $l \in \mathbb{R}^2$, the speaking style $s \in \mathbb{R}^n$ and the character template $Y_c \in \mathbb{R}^{V \times 3}$, where n is the number of speaking styles, T is the length of the mesh sequence, and V is the number of mesh vertices. The emotion level and the speaking style are encoded as one-hot vectors.

Inspired by [Ji *et al.*, 2021] and [Peng *et al.*, 2023b], we use a similar emotion-content disentanglement module that uses pre-trained speech feature extractors wav2vec2.0 [Baezski *et al.*, 2020] to reduce the difficulty of learning the mapping between speech and emotional facial expressions. Specifically, the emotion branch and the content branch firstly disentangle emotion-related features F_e and content-related features F_c from the speech sequence $A_{1:T}$. Then, emotion-related features F_e and content-related features F_c drive the given template vertices to generate offsets $\Delta M_{1:T}^e = (\Delta m_1^e, \Delta m_2^e, \dots, \Delta m_T^e)$ and $\Delta M_{1:T}^c = (\Delta m_1^c, \Delta m_2^c, \dots, \Delta m_T^c)$, respectively, using the same transformer decoder as FaceFormer, which contains a multi-head

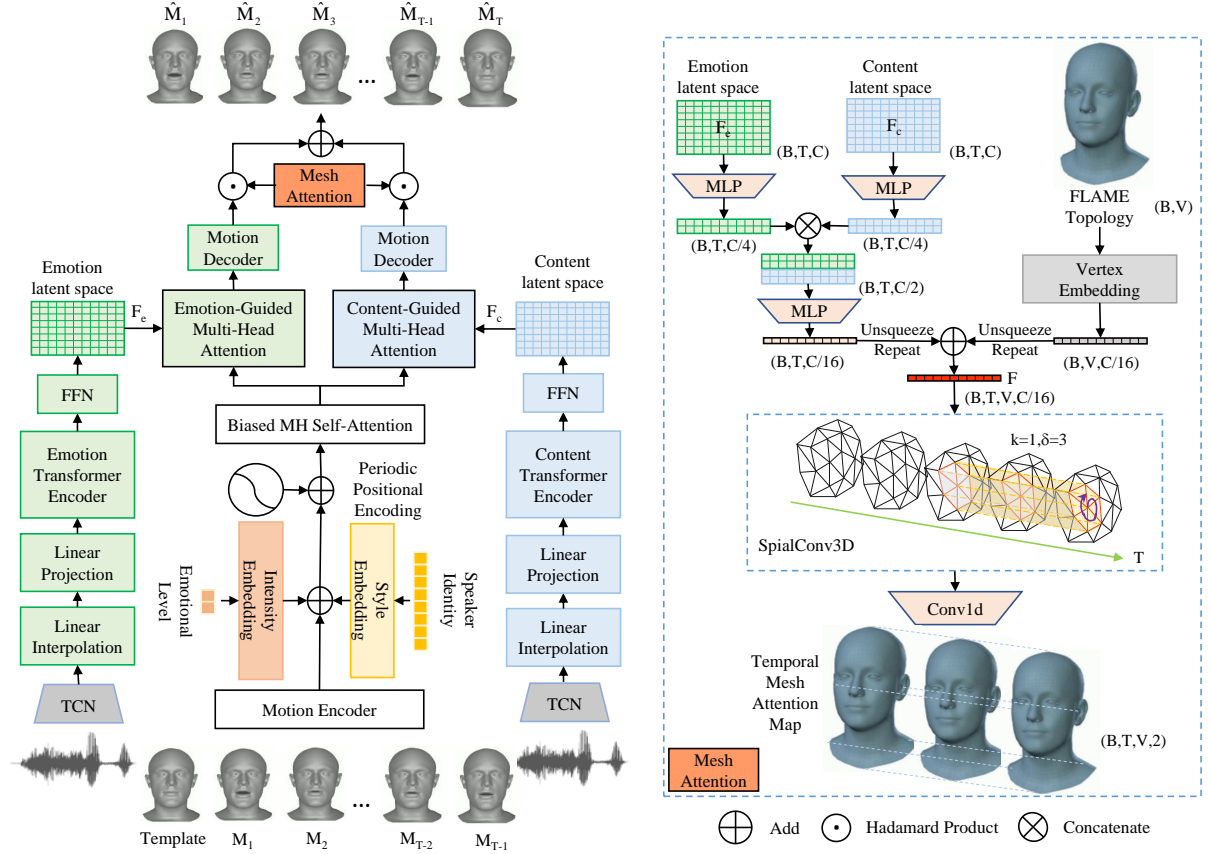


Figure 1: The overall framework of EmoFace. The emotion and content branches disentangle the information in speech, while Mesh Attention fuses these two branches to obtain the final result. The entire framework is end-to-end, thus allowing for efficient training and inference. \hat{M}_i denotes the i -th predicted motion and M_i denotes the i -th reference motion. k and δ represent the spatial neighbourhood and the temporal neighbourhood of SpiralConv3D respectively.

cross-attention module to align the audio and motion modalities as well as a multi-head self-attention module to learn the dependencies between each frame of the past facial motions. Finally, Mesh Attention is provided to fuse the predictions of the two branches in temporal and spatial domains to obtain the final prediction $\Delta M_{1:T}$.

3.2 Mesh Attention

In order to fuse the prediction results of the emotion branch and content branch, we propose a novel spatio-temporal attention module Mesh Attention, as shown in Figure 1. Mesh Attention analyses the emotion features and content features to get the weight of both features. Firstly, $F_{e1} \in \mathbb{R}^{B \times T \times C}$ and $F_{c1} \in \mathbb{R}^{B \times T \times C}$ go through one layer of MLP to get $F_{e1} \in \mathbb{R}^{B \times T \times C/4}$ and $F_{c1} \in \mathbb{R}^{B \times T \times C/4}$ with lower channel dimensions, and then they are concatenated in channel dimensions, followed by another layer of MLP to further reduce the channel number to get the fusion feature $F_{audio} \in \mathbb{R}^{B \times T \times C/16}$. Secondly, we perform the vertex position embedding of the FLAME topology to obtain the position embedding feature $F_{vertices_emb} \in \mathbb{R}^{B \times V \times C/16}$. Furthermore, to obtain the temporal features of the mesh vertices, we integrate the fusion feature F_{audio} and the position embedding

feature $F_{vertices_emb}$. Specifically, the fusion feature F_{audio} is unsqueezed in the second dimension and then repeated V times to obtain $F'_{audio} \in \mathbb{R}^{B \times V \times T \times C/16}$. Similarly, $F_{vertices_emb}$ is unsqueezed in the first dimension and then repeated T times to obtain $F'_{vertices_emb} \in \mathbb{R}^{B \times V \times T \times C/16}$. The obtained features are summed eventually to get the integrated temporal features of the vertices $F \in \mathbb{R}^{B \times V \times T \times C/16}$.

In purpose of further exploring the temporal-spatial connection between the vertices, we design a new graph-based convolution operator, the 3D spiral convolution (SpiralConv3D). In spatial domain, it determines the convolution centre and generates a series of enumerated vertices based on adjacency, followed by 1-ring vertices, 2-ring vertices, and so on, until all vertices containing k rings are included. SpiralConv3D determines the adjacency as follows:

$$\begin{aligned}
 0-ring(v) &= v, \\
 (k+1)-ring(v) &= \mathcal{N}(k-ring(v)) \setminus k-disk(v), \\
 k-disk(v) &= \cup_{i=0, \dots, k} i-ring(v),
 \end{aligned} \tag{1}$$

where $\mathcal{N}(V)$ selects all vertices in the neighborhood of any vertex in set V . In temporal domain, SpiralConv3D considers how the vertices have changed between the past T

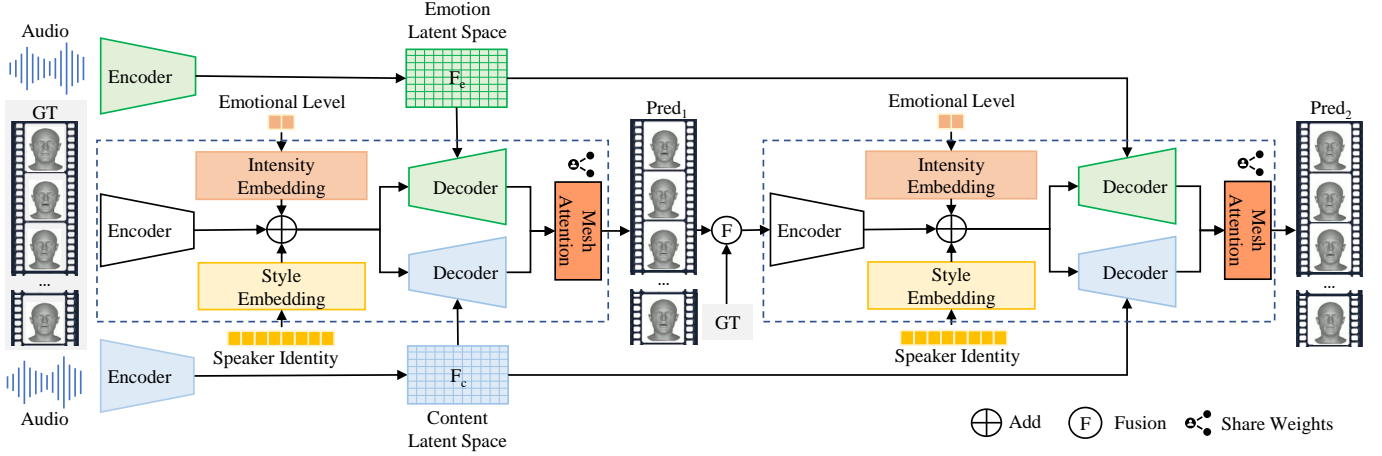


Figure 2: Self-growing scheme. In the first stage, the model inputs all groundtruth frames at once and directly predicts the next frame corresponding to each input frame. In the second stage, the input is changed to a fusion of the groundtruth frames and the predicted frames from the previous stage, and the same prediction process is applied to obtain the final prediction results.

frames, and creates connections to the corresponding vertices between different frames:

$$\text{connect}_\delta(V_{ti}) = \begin{cases} \{V_{t-\delta+1,i}, \dots, V_{t-1,i}, V_{t,i}\}, & t \geq \delta \\ \{\text{Pad}(\delta-t), V_{1,i}, \dots, V_{t,i}\}, & t < \delta \end{cases}, \quad (2)$$

where V_{ti} is the i -th vertex of moment t , $0 \leq t \leq T$ and $0 \leq i \leq 5023$. Meanwhile, $\text{connect}_\delta(V_{ti})$ denotes the connection between V_{ti} and the vertices of past δ frames, and padding is used when $t < \delta$. Similar to 3D ConvNets [Tran *et al.*, 2015], SpiralConv3D considers both temporal and spatial correlations. In contrast, SpiralConv3D applies this spatio-temporal modeling to mesh sequences with a sparse spatial distribution and a dense temporal distribution, considering convolution as the use of fully connected layers for feature fusion:

$$\text{SpiralConv3D}(v) = W(f(\text{connect}_\delta(k\text{-disk}(v)))) + b, \quad (3)$$

where f denotes the feature extractor, W and b are learnable weights and bias. To our knowledge, this work exploits 3D GraphConv in the context of supervised training datasets and modern deep architectures to achieve the best performance on 3D facial animation.

3.3 Training and Testing

Self-growing Scheme

During the training phase, we adopt a novel self-growing scheme instead of teacher-forcing or autoregression scheme, as shown in Figure 2. Self-growing scheme divides the training process in each epoch into two stages. In the first stage, the model inputs all groundtruth frames at once, and then uses Temporal Bias [Fan *et al.*, 2022] to eliminate the influence of future frames and directly predicts the next frame corresponding to each input frame. In the second stage, the model adopts the fusion strategy to obtain new input data and repeats the prediction operation in the previous stage. The fusion strategy is adapted according to the training process. Specifically,

in the first few θ epochs, we keep all the groundtruth frames GT as inputs; in the remaining epochs, the first half gradually replace the groundtruth frames GT with the predicted frames P from the previous stage using the cosine function, and the second half directly abandon the groundtruth frames. The fusion strategy can be denoted as follows:

$$I(n, t) = \begin{cases} GT_t, & n < \theta \text{ or } \text{rand}() < \cos(\frac{\pi(n-\theta)}{N-\theta}) \\ P_t, & n > \frac{(N+\theta)}{2} \text{ or } \text{rand}() \geq \cos(\frac{\pi(n-\theta)}{N-\theta}) \end{cases}, \quad (4)$$

where n and t denote the n -th epoch and the t -th frame, respectively. N means the total number of epochs and $\text{rand}()$ generates a random number from a uniform distribution over the interval $[0, 1]$. Self-growing scheme fully guides in the initial epochs and then gradually reduces the guidance and accepts its own outputs, which weakens the impact of error accumulation and improves the robustness and generation quality.

During inference, EmoFace autoregressively predicts the mesh sequence corresponding to previous 3D talking faces. Specifically, at each moment t , EmoFace predicts the face motion M_t conditioned on the raw audio A , the prior sequence of face motions $M_{\leq t}$, the speaking style s_n , and the emotion level l_n at each moment. The s_n and l_n are determined by the speaker, and thus altering the one-hot identity and intensity vectors can manipulate the output in different styles and emotional levels.

Supervision Training Strategy of Emotion-Content Disentanglement Module

We set a pseudo-training pair of samples with the same content but different emotions. The emotion features and content features are extracted respectively and the two emotion features are exchanged as input of transformer decoder to implement cross reconstruction. Since that we expect both the emotion branch and the content branch to be as strong

Subject	Gender Ratio	Text	Emotion	Sentence	FPS	Topology	Training:Validation:Testing
24	1:1	60	8	1440	30	FLAME	10:1:1

Table 1: Statistics of 3D-RAVDESS dataset.

as possible in modeling the speech-mesh mapping relationship, our emotion branch and content branch make separate predictions for the mesh offsets of the next frame. We incorporate the intermediate supervision into the predictions of two separate branches. However, both branches have significant limitations in their respective abilities to model facial motions. On the one hand, although the features extracted from the content branch are strongly correlated with the lips, the inability to extract long-term emotional features and the lack of the type and intensity of emotion are not conducive to predicting the magnitude of mouth opening. On the other hand, though the features extracted from the emotion branch are strongly correlated with the motions of the eyes and the face expressions, the lack of short-term content features results in insufficiently accurate predictions of the lips. Thus, as mentioned before, Mesh Attention is designed to fuse the driving results of the two branches in temporal and spatial domains to obtain the final prediction. Our self-reconstruction loss, cross-reconstruction loss, velocity loss and classification loss are as follows:

$$L_{self} = \left\| M_{c1,e1}^e - \hat{M}_{c1,e1} \right\|_1 + \left\| M_{c1,e1}^c - \hat{M}_{c1,e1} \right\|_1 + \left\| M_{c1,e1} - \hat{M}_{c1,e1} \right\|_1, \quad (5)$$

$$L_{cross} = \left\| M_{c1,e2}^e - \hat{M}_{c1,e2} \right\|_1 + \left\| M_{c1,e2}^c - \hat{M}_{c1,e2} \right\|_1 + \left\| M_{c1,e2} - \hat{M}_{c1,e2} \right\|_1, \quad (6)$$

$$L_{vel} = \left\| M_{c1,e1}^t - M_{c1,e1}^{t-1}, \hat{M}_{c1,e1}^t - \hat{M}_{c1,e1}^{t-1} \right\|_1 + \left\| M_{c1,e2}^t - M_{c1,e2}^{t-1}, \hat{M}_{c1,e2}^t - \hat{M}_{c1,e2}^{t-1} \right\|_1, \quad (7)$$

$$L_{cls} = - \sum_i \sum_{\phi=1}^{N_e} (y_{i\phi} * \log p_{i\phi}), \quad (8)$$

where $M_{cx,ey}$ represents predicted mesh sequence with content x and emotion y . M^c and M^e represents predicted mesh sequence of content branch and emotion branch, respectively. M^t means the t -th frame of mesh sequence, \hat{M} means the groundtruth, N_e represents the number of distinct emotion categories, $y_{i\phi}$ is the observation function that determines whether sample i carries the emotion label ϕ , and $p_{i\phi}$ denotes the predicted probability that sample i belongs to class ϕ . Note that the first two terms of self-reconstruction loss and cross-reconstruction loss are intermediate supervision of the two branches. The overall function is given by:

$$L_1 = \lambda_1 L_{self} + \lambda_2 L_{cross} + \lambda_3 L_{vel} + \lambda_4 L_{class}, \quad (9)$$

where $\lambda_1 = \lambda_2 = 1000$, $\lambda_3 = 500$ and $\lambda_4 = 0.0001$ in all of our experiments.

Methods	VOCASET		3D-RAVDESS	
	LVE ↓	EVE ↓	LVE ↓	EVE ↓
VOCA [2019]	4.9245	–	–	–
MeshTalk [2021]	4.5441	–	–	–
FaceFormer [2022]	4.1090	0.4858	5.8462	1.4149
CodeTalker [2023]	3.9445	0.5074	15.6160	3.4675
EmoTalk [2023b]	3.7798	0.4862	6.6076	1.5994
SelfTalk [2023a]	3.2238	0.4562	6.2560	1.5685
TalkingStyle [2024]	3.5245	0.4686	5.9737	1.4471
EmoFace(Ours)	2.8669	0.4664	4.8863	0.9509

Table 2: Quantitative evaluation results on VOCASET and 3D-RAVDESS.(For better visualization, we scale up the LVE and EVE by a factor of 10^{-5} .)

4 Experiments

4.1 Experimental Settings

We employ two datasets, including the non-emotional dataset VOCASET and the emotional dataset 3D-RAVDESS, where the 3D-RAVDESS dataset is the dataset we constructed.

VOCASET dataset. VOCASET [Cudeiro *et al.*, 2019] consists of 480 face mesh sequences from 12 subjects. Each mesh sequence is 60fps and is between 3 and 4 seconds long in duration. Meanwhile, each 3D face mesh has 5023 vertices. We follow the data configuration of VOCA for a fair comparison.

3D-RAVDESS Dataset. The RAVDESS [Livingstone and Russo, 2018] is a multimodal emotion recognition dataset. As shown in Table 1, the dataset contains 24 actors (12 male and 12 female), each actor has 60 sentences with a total of 1440 face mesh sequences and corresponding speech. Each actor in this dataset provides data on different emotion categories and emotion levels, including neutral, calm, happy, sad, angry, fearful, disgusted, and surprised. In this case, the data corresponding to the first 20 subjects of the dataset are used for training, the 21st and 22nd subjects are used for validation, and the last two subjects are used for testing. We first process 1440 videos from the original RAVDESS dataset to convert the frame rate to 30 fps. Then, the emotional 3D faces are reconstructed using EMOCA [Daněček *et al.*, 2022] to obtain a sequence of 5023 mesh vertices under the FLAME network topology. Due to the jittery results, we use Kalman Filter [Kalman, 1960] on the FLAME parameters and fix the last three of the pose parameters to obtain 3D head mesh sequences with smooth front view. Our 3D-RAVDESS dataset consists of these mesh sequences and the corresponding speech from the original 2D dataset.

4.2 Quantitative evaluation

To evaluate the lip synchronisation, we compute the lip vertex error (LVE) that is used in previous work [Fan *et al.*, 2022]. This metric computes the maximum ℓ_2 error among all lip

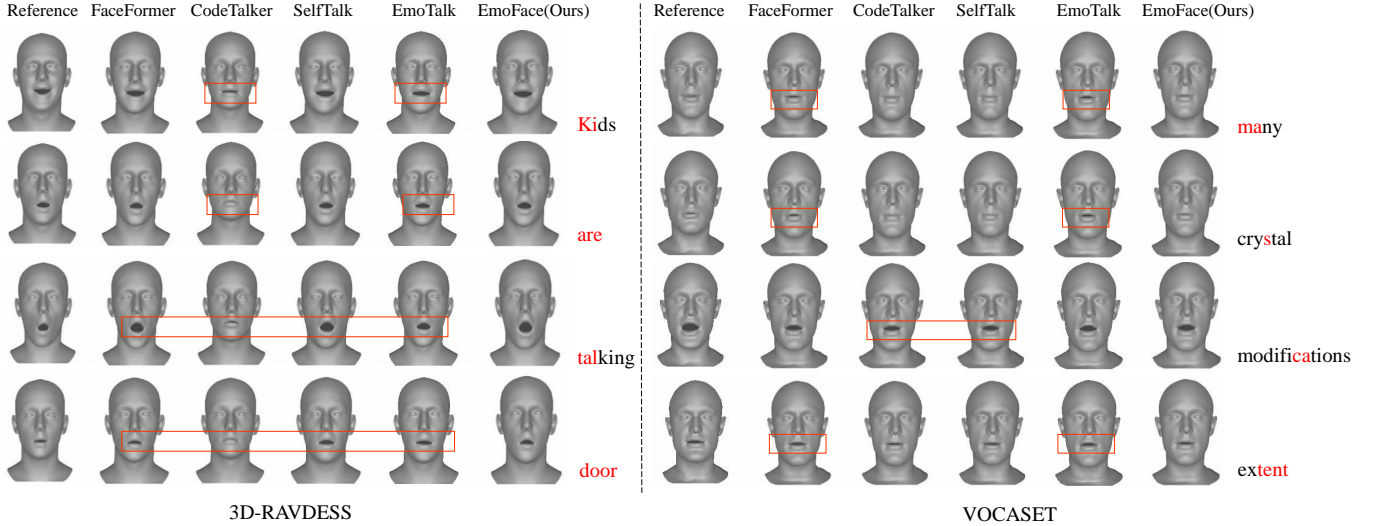


Figure 3: Qualitative comparison of the facial movements of the different methods on 3D-RAVDESS (top) and VOCASET (bottom). On 3D-RAVDESS, we generate facial animations of saying the sentence “Kids are talking by the door.” with surprised. On VOCA-Test, we generate facial animations of saying the sentence “How many crystal modifications of uranium hydride are extent?” without emotion. Significant differences in the lip region are denoted by red boxes. EmoFace generates more realistic facial movements that match the speech, whether it’s emotional or not.

vertices in the test set and averages ℓ_2 error across all frames. Additionally, the emotional vertex error (EVE) [Peng *et al.*, 2023b] is used to reflect the full emotional expression. It measures the maximum ℓ_2 error of all eye and forehead vertices in the test set and averages ℓ_2 error of them. Table 2 demonstrates significant advantages of our algorithm in handling emotional speech-driven 3D face. In particular, our LVE and EVE on 3D-RAVDESS dataset is 20% and 35% lower than SelfTalk, respectively.

4.3 Qualitative evaluation

We qualitatively compare the driving effects of cross-identity between different models by driving the new 3D character templates in the test set with the speaking style of the training characters. The left side of Figure 3 shows the driving results of different models for the same speech with strong surprised emotion, and the right side shows the driving results of different models in non-emotional speech. Since that the speaking style of the new characters is unknown in the test data, the model may be driven slightly differently to the real results. In terms of lip synchronisation, EmoFace shows a greater amplitude of movement, which is particularly evident in the lip shapes for “are”, “talking” and “door”. This provides a more accurate reflection of surprise and is more consistent with real movements of the lips. In addition, it also has a higher degree of mouth closure than other methods, for example, when pronouncing “many”, “crystal” and “extent”. Furthermore, the full face comparison in Figure 3 indicates that EmoFace drives more obvious and natural expressions. To further demonstrate the superiority of our algorithm for both emotional and non-emotional audio inputs, a supplementary video is provided for more detailed comparisons.

Modules	LVE ($\times 10^{-5}$ mm)	EVE ($\times 10^{-5}$ mm)
w/o self-growing	5.3898	1.6794
w/o Mesh Attention	10.7420	1.0965
Ours	4.8863	0.9509

Table 3: Ablation study for our components. We show the LVE and EVE in different cases.

4.4 Ablation experiments

In this section, we conduct ablation experiments to investigate the impact of our training strategy and Mesh Attention. All ablation experiments are conducted on the 3D-RAVDESS dataset.

Impact of self-growing scheme.

We train our method using teacher-forcing without self-growing and obtain higher LVE and EVE, as shown in Table 3. We believe the reason is that guiding is too strong, leading to poor robustness, and the prediction errors in the previous frames accumulate and affect the subsequent frames. However, with a gradually weakened guiding in the self-growing scheme, EmoFace is trained to take the errors of the previous frames into account, which is similar to the situation during inference.

Impact of Mesh Attention.

We compare the difference in effectiveness between the Mesh Attention module and the Add operation. Table 3 also demonstrates that directly adding up the gains predicted by the two branches without Mesh Attention leads to a great degradation of model performance, whereas a weighted sum seems more reasonable. This indicates that the contribution of the two branches differs in the different head regions.

Dilation	Kernel Size	Time Duration	LVE ($\times 10^{-5}$ mm)	EVE ($\times 10^{-5}$ mm)
1	5	3	5.3472	1.1495
1	9	3	5.2177	1.1089
1	18	3	4.7527	1.0244
2	18	3	4.8863	0.9509
4	18	3	5.1323	1.1390
2	18	1	5.3476	1.1715
2	18	2	5.5372	1.2144

Table 4: Ablation study of SpiralConv3D.

Methods	full face realism	lip synchronization	eye movement	emotion expression
FaceFormer	3.3	3.3	3.0	3.2
CodeTalker	2.6	2.4	2.3	2.4
EmoTalk	3.5	3.2	3.6	3.9
SelfTalk	3.7	3.6	3.6	3.8
EmoFace	4.0	3.9	3.9	3.9

Table 5: User study results.

Hyperparameters of SpiralConv3D.

A series of ablation experiments on dilation, kernel size and time duration are provided, as shown in Table 4. In terms of dilation coefficients, the third to fifth rows show that proper dilation can improve performance, while excessive dilation leads to performance degradation. SpiralConv3D may under-consider nearby vertex features with too large dilation coefficient. Furthermore, with respect to kernel size, the first to third rows indicate that large convolution kernels bring high generation quality. SpiralConv3D with a larger kernel size integrates vertex features within a larger spatial receptive field, which has a significant effect on the performance improvement. Finally, the fourth and the last two rows demonstrate the importance of large temporal receptive field. A larger time duration means that the connectivity relationship of the vertices between more video frames are considered. Time duration coefficient of 1 degrades SpiralConv3D to SpiralConv2D, which only spatially fuses the features and performs worse than configuration of the fourth row. Based on the results of the quantitative comparison, we adopt the configuration of the fourth row.

4.5 Visualization

We believe that although the lips are directly controlled by the content of the speech, the gain from emotion is also quite important. Hence, we visualize the attention weight of the emotion branch with darker colour representing larger weights, as shown in Figure 4. It is obvious that emotion brings great effects on the amplitude and direction of movements in the mouth, jaw and eye regions. In other words, these regions are strongly correlative to emotion.

In the Supplementary Video, we visualize the animation demo of the content branch. It performs normally in non-silent frames but shows obvious lip jitter in silent frames, thus also resulting in unstable output of the Addition. However, EmoFace dynamically combines the two branches with Mesh Attention to obtain better animation results in terms of lip

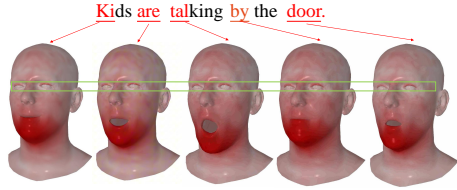


Figure 4: Visualization of the importance of emotional information for facial regions. The eyes, mouth and jaw are strongly correlated with emotions.

synchronization, expression synchronization, movement amplitude and coherence.

More results under VOCASET-Test, 3D-RAVDESS-Test and long speech in the wild, performance on different emotions and comparative demonstrations of ablation experiments are shown in the Supplementary Video.

4.6 User study

We design a comprehensive research questionnaire to evaluate the effectiveness of EmoFace and compare it with FaceFormer, CodeTalker, EmoTalk and SelfTalk. We provide 12 sets of comparison results on 3D-RAVDESS-Test and VOCA-Test with 8 emotions, and finally make 48 questions targeting four aspects: full face realism, lip synchronization, eye movement and emotion expression. The questionnaire shows comparison videos to the respondents and asks them to rate the effectiveness of each algorithm. We calculate the Mean Opinion Score (MOS) of all methods and EmoFace obtains the highest MOS, suggesting that our method receives the most positive feedback.

5 Conclusion and Discussion

In this paper, we present EmoFace, an emotional speech-driven 3D talking face model. Our model disentangles the emotion and content from the speech and predicts the mesh offsets driven by emotion and content, respectively. To further improve the prediction accuracy, new Mesh Attention integrates the output mesh offsets. Particularly, a novel graph-based SpiralConv3D is adopted to fuse spatio-temporal features of mesh sequences. Extensive experiments conducted under self-growing scheme using both public dataset VOCASET and newly constructed high-quality dataset 3D-RAVDESS demonstrate that our model outperforms existing state-of-the-art methods and receives better user experience feedback.

Although our model gets state-of-the-art results, there are still some limitations to address in future work. On the one hand, speech driven methods do not model expressions and motions that are unrelative to audio, for example, eye blinks. Our next work will take the video input into account to obtain better animation results. On the other hand, the Mesh Attention proposed in our work meets large amount of computation because of the 3D spiral convolution operator. More explorations will be done to reduce the computation costs.

Ethical Statement

Face data can be used for generating content that may jeopardize privacy. We must act responsibly by considering the aspects related to privacy and ethics.

References

[Baevski *et al.*, 2020] Alexei Baevski, Yuhao Zhou, Abdelrahman Mohamed, and Michael Auli. wav2vec 2.0: A framework for self-supervised learning of speech representations. *Advances in neural information processing systems*, 33:12449–12460, 2020.

[Chen *et al.*, 2023] Peng Chen, Xiaobao Wei, Ming Lu, Yitong Zhu, Naiming Yao, Xingyu Xiao, and Hui Chen. Diffusiontalker: Personalization and acceleration for speech-driven 3d face diffuser. *arXiv preprint arXiv:2311.16565*, 2023.

[Cudeiro *et al.*, 2019] Daniel Cudeiro, Timo Bolkart, Cassidy Laidlaw, Anurag Ranjan, and Michael J Black. Capture, learning, and synthesis of 3d speaking styles. In *Proceedings of the IEEE/CVF Conference on Computer Vision and Pattern Recognition*, pages 10101–10111, 2019.

[Daněček *et al.*, 2022] Radek Daněček, Michael J Black, and Timo Bolkart. Emoca: Emotion driven monocular face capture and animation. In *Proceedings of the IEEE/CVF Conference on Computer Vision and Pattern Recognition*, pages 20311–20322, 2022.

[Daněček *et al.*, 2023] Radek Daněček, Kiran Chhatre, Shashank Tripathi, Yandong Wen, Michael Black, and Timo Bolkart. Emotional speech-driven animation with content-emotion disentanglement. In *SIGGRAPH Asia 2023 Conference Papers*, pages 1–13, 2023.

[Defferrard *et al.*, 2016] Michaël Defferrard, Xavier Bresson, and Pierre Vandergheynst. Convolutional neural networks on graphs with fast localized spectral filtering. *Advances in neural information processing systems*, 29, 2016.

[Edwards *et al.*, 2016] Pif Edwards, Chris Landreth, Eugene Fiume, and Karan Singh. Jali: an animator-centric viseme model for expressive lip synchronization. *ACM Transactions on graphics (TOG)*, 35(4):1–11, 2016.

[Ekman and Friesen, 1978] Paul Ekman and Wallace V Friesen. Facial action coding system. *Environmental Psychology & Nonverbal Behavior*, 1978.

[Fan *et al.*, 2022] Yingruo Fan, Zhaojiang Lin, Jun Saito, Wenping Wang, and Taku Komura. Faceformer: Speech-driven 3d facial animation with transformers. In *Proceedings of the IEEE/CVF Conference on Computer Vision and Pattern Recognition*, pages 18770–18780, 2022.

[Gong *et al.*, 2019] Shunwang Gong, Lei Chen, Michael Bronstein, and Stefanos Zafeiriou. Spiralnet++: A fast and highly efficient mesh convolution operator. In *Proceedings of the IEEE/CVF international conference on computer vision workshops*, pages 0–0, 2019.

[Ji *et al.*, 2021] Xinya Ji, Hang Zhou, Kaisiyuan Wang, Wayne Wu, Chen Change Loy, Xun Cao, and Feng Xu. Audio-driven emotional video portraits. In *Proceedings of the IEEE/CVF conference on computer vision and pattern recognition*, pages 14080–14089, 2021.

[Kalman, 1960] Rudolph Emil Kalman. A new approach to linear filtering and prediction problems. 1960.

[Karras *et al.*, 2017] Tero Karras, Timo Aila, Samuli Laine, Antti Herva, and Jaakko Lehtinen. Audio-driven facial animation by joint end-to-end learning of pose and emotion. *ACM Transactions on Graphics (TOG)*, 36(4):1–12, 2017.

[Kulon *et al.*, 2020] Dominik Kulon, Riza Alp Guler, Iasonas Kokkinos, Michael M Bronstein, and Stefanos Zafeiriou. Weakly-supervised mesh-convolutional hand reconstruction in the wild. In *Proceedings of the IEEE/CVF conference on computer vision and pattern recognition*, pages 4990–5000, 2020.

[Lahiri *et al.*, 2021] Avisek Lahiri, Vivek Kwatra, Christian Frueh, John Lewis, and Chris Bregler. Lipsync3d: Data-efficient learning of personalized 3d talking faces from video using pose and lighting normalization. In *Proceedings of the IEEE/CVF conference on computer vision and pattern recognition*, pages 2755–2764, 2021.

[Li *et al.*, 2017] Tianye Li, Timo Bolkart, Michael J Black, Hao Li, and Javier Romero. Learning a model of facial shape and expression from 4d scans. *ACM Trans. Graph.*, 36(6):194–1, 2017.

[Lim *et al.*, 2018] Isaak Lim, Alexander Dielen, Marcel Campen, and Leif Kobbelt. A simple approach to intrinsic correspondence learning on unstructured 3d meshes. In *Proceedings of the European conference on computer vision (ECCV) workshops*, pages 0–0, 2018.

[Livingstone and Russo, 2018] Steven R Livingstone and Frank A Russo. The ryerson audio-visual database of emotional speech and song (ravdess): A dynamic, multimodal set of facial and vocal expressions in north american english. *PloS one*, 13(5):e0196391, 2018.

[Masci *et al.*, 2015] Jonathan Masci, Davide Boscaini, Michael Bronstein, and Pierre Vandergheynst. Geodesic convolutional neural networks on riemannian manifolds. In *Proceedings of the IEEE international conference on computer vision workshops*, pages 37–45, 2015.

[Mattheyses and Verhelst, 2015] Wesley Mattheyses and Werner Verhelst. Audiovisual speech synthesis: An overview of the state-of-the-art. *Speech Communication*, 66:182–217, 2015.

[Mihaylova and Martins, 2019] Tsvetomila Mihaylova and André F. T. Martins. Scheduled sampling for transformers. In *Proceedings ACL SRW*, 2019.

[Peng *et al.*, 2023a] Ziqiao Peng, Yihao Luo, Yue Shi, Hao Xu, Xiangyu Zhu, Hongyan Liu, Jun He, and Zhaoxin Fan. Selftalk: A self-supervised commutative training diagram to comprehend 3d talking faces. In *Proceedings of the 31st ACM International Conference on Multimedia*, pages 5292–5301, 2023.

[Peng *et al.*, 2023b] Ziqiao Peng, Haoyu Wu, Zhenbo Song, Hao Xu, Xiangyu Zhu, Jun He, Hongyan Liu, and Zhaoxin Fan. Emotalk: Speech-driven emotional disentanglement for 3d face animation. In *Proceedings of the IEEE/CVF International Conference on Computer Vision (ICCV)*, pages 20687–20697, October 2023.

[Pham *et al.*, 2017] Hai X Pham, Samuel Cheung, and Vladimir Pavlovic. Speech-driven 3d facial animation with implicit emotional awareness: A deep learning approach. In *Proceedings of the IEEE conference on computer vision and pattern recognition workshops*, pages 80–88, 2017.

[Ping *et al.*, 2013] Heng Yu Ping, Lili Nurliyana Abdullah, Puteri Suhaiza Sulaiman, and Alfian Abdul Halin. Computer facial animation: A review. *International Journal of Computer Theory and Engineering*, 5(4):658, 2013.

[Richard *et al.*, 2021] Alexander Richard, Michael Zollhöfer, Yandong Wen, Fernando De la Torre, and Yaser Sheikh. Meshtalk: 3d face animation from speech using cross-modality disentanglement. In *Proceedings of the IEEE/CVF International Conference on Computer Vision*, pages 1173–1182, 2021.

[Song *et al.*, 2024] Wenfeng Song, Xuan Wang, Shi Zheng, Shuai Li, Aimin Hao, and Xia Hou. Talkingstyle: Personalized speech-driven 3d facial animation with style preservation. *IEEE Transactions on Visualization and Computer Graphics*, pages 1–12, 2024.

[Stan *et al.*, 2023] Stefan Stan, Kazi Injamamul Haque, and Zerrin Yumak. Facediffuser: Speech-driven 3d facial animation synthesis using diffusion. In *Proceedings of the 16th ACM SIGGRAPH Conference on Motion, Interaction and Games*, pages 1–11, 2023.

[Sun *et al.*, 2024] Zhiyao Sun, Tian Lv, Sheng Ye, Matthieu Lin, Jenny Sheng, Yu-Hui Wen, Minjing Yu, and Yong-Jin Liu. Diffposetalk: Speech-driven stylistic 3d facial animation and head pose generation via diffusion models. *ACM Transactions on Graphics (TOG)*, 43(4), 2024.

[Taylor *et al.*, 2017] Sarah Taylor, Taehwan Kim, Yisong Yue, Moshe Mahler, James Krahe, Anastasio Garcia Rodriguez, Jessica Hodgins, and Iain Matthews. A deep learning approach for generalized speech animation. *ACM Transactions On Graphics (TOG)*, 36(4):1–11, 2017.

[Tran *et al.*, 2015] Du Tran, Lubomir Bourdev, Rob Fergus, Lorenzo Torresani, and Manohar Paluri. Learning spatiotemporal features with 3d convolutional networks. In *Proceedings of the IEEE international conference on computer vision*, pages 4489–4497, 2015.

[Van Den Oord *et al.*, 2017] Aaron Van Den Oord, Oriol Vinyals, et al. Neural discrete representation learning. *Advances in neural information processing systems*, 30, 2017.

[Vaswani *et al.*, 2017] Ashish Vaswani, Noam Shazeer, Niki Parmar, Jakob Uszkoreit, Llion Jones, Aidan N Gomez, Łukasz Kaiser, and Illia Polosukhin. Attention is all you need. *Advances in neural information processing systems*, 30, 2017.

[Wohlgenannt *et al.*, 2020] Isabell Wohlgenannt, Alexander Simons, and Stefan Stieglitz. Virtual reality. *Business & Information Systems Engineering*, 62:455–461, 2020.

[Wu *et al.*, 2023] Haozhe Wu, Songtao Zhou, Jia Jia, Junliang Xing, Qi Wen, and Xiang Wen. Speech-driven 3d face animation with composite and regional facial movements. In *Proceedings of the 31st ACM International Conference on Multimedia*, pages 6822–6830, 2023.

[Xing *et al.*, 2023] Jinbo Xing, Menghan Xia, Yuechen Zhang, Xiaodong Cun, Jue Wang, and Tien-Tsin Wong. Codetalker: Speech-driven 3d facial animation with discrete motion prior. In *Proceedings of the IEEE/CVF Conference on Computer Vision and Pattern Recognition*, pages 12780–12790, 2023.

[Xu *et al.*, 2013] Yuyu Xu, Andrew W Feng, Stacy Marsella, and Ari Shapiro. A practical and configurable lip sync method for games. In *Proceedings of Motion on Games*, pages 131–140. 2013.